Unconventional Topological Phase Transition in Two-Dimensional Systems with Space-Time Inversion Symmetry

Junyeong Ahn[1,2,3] and Bohm-Jung Yang[1,2,3*]
[1]Department of Physics and Astronomy, Seoul National University, Seoul 08826, Korea
[2]Center for Correlated Electron Systems, Institute for Basic Science (IBS), Seoul 08826, Korea
[3]Center for Theoretical Physics (CTP), Seoul National University, Seoul 08826, Korea
(Received 28 September 2016; revised manuscript received 1 February 2017; published 10 April 2017)

We study a topological phase transition between a normal insulator and a quantum spin Hall insulator in two-dimensional (2D) systems with time-reversal and twofold rotation symmetries. Contrary to the case of ordinary time-reversal invariant systems, where a direct transition between two insulators is generally predicted, we find that the topological phase transition in systems with an additional twofold rotation symmetry is mediated by an emergent stable 2D Weyl semimetal phase between two insulators. Here the central role is played by the so-called space-time inversion symmetry, the combination of time-reversal and twofold rotation symmetries, which guarantees the quantization of the Berry phase around a 2D Weyl point even in the presence of strong spin-orbit coupling. Pair creation and pair annihilation of Weyl points accompanying partner exchange between different pairs induces a jump of a 2D Z_2 topological invariant leading to a topological phase transition. According to our theory, the topological phase transition in HgTe/CdTe quantum well structure is mediated by a stable 2D Weyl semimetal phase because the quantum well, lacking inversion symmetry intrinsically, has twofold rotation about the growth direction. Namely, the HgTe/CdTe quantum well can show 2D Weyl semimetallic behavior within a small but finite interval in the thickness of HgTe layers between a normal insulator and a quantum spin Hall insulator. We also propose that few-layer black phosphorus under perpendicular electric field is another candidate system to observe the unconventional topological phase transition mechanism accompanied by the emerging 2D Weyl semimetal phase protected by space-time inversion symmetry.

DOI: 10.1103/PhysRevLett.118.156401

Introduction.—Symmetry-protected topological phases have become a quintessential notion in condensed matter physics, after the discovery of time-reversal invariant topological insulators [1–3] and topological crystalline insulators [4]. Although the importance of symmetry to protect bulk topological properties is widely recognized, relatively little attention has been given to understanding the role of symmetry for the description of topological phase transition (TPT). Early studies on this issue have focused on time-reversal T and inversion P, and have shown that the nature of TPT in T-invariant three-dimensional (3D) systems changes dramatically depending on the presence or absence of P symmetry [5]. Namely, when the system has both T and P symmetries, a direct transition between a normal insulator (NI) and a Z_2 topological insulator is possible when a band inversion happens between two bands with opposite parities. This is in contrast to noncentrosymmetric systems lacking P, where the transition between a NI and a topological insulator is generally mediated by a 3D Weyl semimetal (WSM) phase in between. The intermediate stable semimetal phase can appear when the following two conditions are satisfied. First, the codimension analysis for accidental band crossing at a generic momentum should predict a group of gapless solutions. Second, a gapless point in the semimetal phase should carry a quantized topological invariant guaranteeing its stability.

In contrast to 3D, in two dimensions the codimension analysis [6] predicts that there is always a direct transition between a NI and a quantum spin Hall insulator (QSHI) even in noncentrosymmetric systems [see Fig. 1(a)]. The reason is that in a generic 2D system with a single tuning parameter m (representing pressure, doping, etc.), an effective 2×2 Hamiltonian describing band crossing depends on three independent variables (k_x, k_y, m) including two momenta k_x and k_y. To achieve a band crossing, however, because the coefficients of three Pauli matrices associated with the effective 2×2 Hamiltonian should vanish by adjusting three variables, only a single gap-closing solution can be

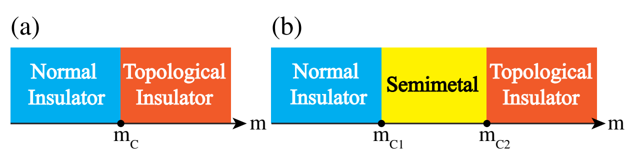

FIG. 1. Schematic phase diagram for a topological phase transition in a time-reversal invariant 2D noncentrosymmetric system. (a) Systems with only time-reversal symmetry. (b) Systems with an additional twofold rotation symmetry about an axis perpendicular to the 2D plane.

found. This unique gap-closing solution describes the critical point for a direct transition between two gapped insulators. The absence of a stable semimetal phase mediating the transition between two insulators is consistent with the fact that a gap-closing point does not carry a topological invariant in a generic T-invariant 2D system in the presence of spin-orbit coupling.

In this Letter, we show that the TPT between a NI and a QSHI is always mediated by an emerging 2D Weyl [7] semimetal [see Fig. 1(b)], when a T-invariant noncentrosymmetric 2D system is invariant under twofold rotation C_{2z} about an axis perpendicular to the 2D plane. The intermediate 2D WSM is stable due to the π Berry phase around a Weyl point (WP), which is quantized even in the presence of spin-orbit coupling. Here the central role is played by the so-called space-time inversion I_{ST} which is nothing but the combination of T and C_{2z}; i.e., $I_{\mathrm{ST}} = C_{2z}T$. Since I_{ST} ensures the quantization of the Berry phase around a 2D WP, the transition between an insulator and a WSM is accompanied by pair creation and pair annihilation of 2D WPs. Moreover, partner exchange between pairs of WPs can induce the change of the Z_2 topological invariant; thus, the 2D WSM can mediate a TPT. We propose two candidate materials where the unconventional TPT mediated by a 2D WSM can be realized. One is the HgTe/CdTe quantum well where inversion is absent intrinsically [8–11] and the TPT can be controlled by changing the thickness of the HgTe layer. We expect that there can be a finite thickness window where a stable 2D WSM appears between a NI and a QSHI. We also propose that the unconventional TPT can be observed in few-layer black phosphorus under vertical electric field.

Band crossing in systems with I_{ST}.—C_{2z} transforms a spatial coordinate (x, y, z) to $(-x, -y, z)$. Because the z coordinate is invariant under C_{2z}, for a layered 2D system with a fixed z, C_{2z} can be considered as an effective inversion symmetry mapping (x, y) to $(-x, -y)$. Thus, in 2D systems, $I_{\mathrm{ST}} = C_{2z}T$ transforms a space-time coordinate (x, y, t) to $(-x, -y, -t)$. In momentum space, on the other hand, it is a local symmetry because the momentum $\boldsymbol{k} = (k_x, k_y)$ remains invariant under I_{ST}. As discussed in Ref. [12], I_{ST} has various intriguing properties. For instance, because Berry curvature $F_{xy}(\boldsymbol{k})$ transforms to $-F_{xy}(\boldsymbol{k})$ under I_{ST}, $F_{xy}(\boldsymbol{k})$ vanishes locally unless there is a singular gapless point, which guarantees the quantization of π Berry phase around a 2D WP. Moreover, since $I_{\mathrm{ST}}^2 = +1$ irrespective of the presence or absence of spin-orbit coupling, it does not require Kramers degeneracy at each $\boldsymbol{k}$. This can be contrasted to the case of PT, satisfying $(PT)^2 = -1(+1)$ in the presence (absence) of spin-orbit coupling. Especially, when $(PT)^2 = -1$, Kramers theorem requires double degeneracy at each $\boldsymbol{k}$. Because Berry phase is not quantized in this case, a Dirac point is unstable [13].

Here we show that I_{ST} also modifies the gap-closing condition in an essential way, leading to an unconventional TPT. Because each band is nondegenerate at a generic momentum $\boldsymbol{k}$ in noncentrosymmetric systems, an accidental band crossing can be described by a 2×2 matrix Hamiltonian $H(\boldsymbol{k}) = f_0(\boldsymbol{k}, m) + \sum_{i=x,y,z} f_i(\boldsymbol{k}, m)\sigma_i$, where $\sigma_{x,y,z}$ indicates the two bands touching near the Fermi level and m describes a tuning parameter such as electric field, pressure, etc. Because I_{ST} is antiunitary, it can generally be represented by $I_{\mathrm{ST}} = UK$, where U is a unitary matrix and K denotes complex conjugation. By choosing a suitable basis, one can obtain $I_{\mathrm{ST}} = K$, as shown in the Supplemental Material [14]. Then, the I_{ST} symmetry requires $H^*(\boldsymbol{k}) = H(\boldsymbol{k})$, which leads to

$$H(\boldsymbol{k}) = f_0(\boldsymbol{k}, m) + f_x(\boldsymbol{k}, m)\sigma_x + f_z(\boldsymbol{k}, m)\sigma_z. \quad (1)$$

Accidental gap-closing can happen if and only if $f_x = f_z = 0$. Because there are three independent variables (k_x, k_y, m) while there are only two equations $f_x = f_z = 0$ to be satisfied, one can expect a line of gapless solutions in (k_x, k_y, m) space, which predicts an emerging 2D stable semimetal [see Fig. 1(b)]. Near the critical point $m = m_{c1}$ where accidental band crossing happens, the Hamiltonian can generally be written as

$$H(\boldsymbol{q}) = (Aq_x^2 + m_{c1} - m)\sigma_x + vq_y\sigma_z, \quad (2)$$

which describes a gapped insulator (a 2D WSM) when $m < m_{c1}$ ($m > m_{c1}$) assuming $A > 0$. Because of T symmetry, accidental band crossing happens at two momenta $\pm\boldsymbol{k}$. Since two WPs are created at each band-crossing point, the WSM has four WPs in total. Moreover, when m becomes larger than m_{c1}, four WPs migrate in momentum space, and eventually they are annihilated pairwise at $m = m_{c2}$. Interestingly, when pair creation and pair annihilation is accompanied by partner switching between WP pairs, the two gapped phases mediated by the WSM should have distinct topological properties as shown below.

Change of Z_2 invariant via pair creation and pair annihilation of 2D WPs.—The Z_2 invariant Δ of a T-invariant 2D system can be written as [21]

$$\Delta = P_T(\pi) - P_T(0) \mod 2, \quad (3)$$

where $P_T(k_x)$ is the time-reversal polarization of a T-invariant one-dimensional (1D) subsystem connecting two time-reversal invariant momenta (TRIM) with given $k_x = 0, \pi$. For instance, Fig. 2(a) shows T-invariant 1D subsystems passing two TRIMs with $k_x = 0$ or $k_x = \pi$, respectively. For such a 1D subsystem, P_T is defined as

$$P_T = P^I - P^{II} = 2P^I - P_\rho, \quad (4)$$

where $P_\rho = P^I + P^{II}$ is the charge polarization, and P^I and P^{II} are the partial polarization associated with the wave function $u_n^I(k)$ and its Kramers partner $u_n^{II}(-k) \propto Tu_n^I(k)$ where n labels occupied bands. Namely, $P^{j=I,II} = \oint (dk/2\pi)A^j(k)$ with $A^j(k) = i\sum_n \langle u_n^j(k)|\nabla_k|u_n^j(k)\rangle$. $P^{j=I,II}$ can also be written as a summation of Wannier

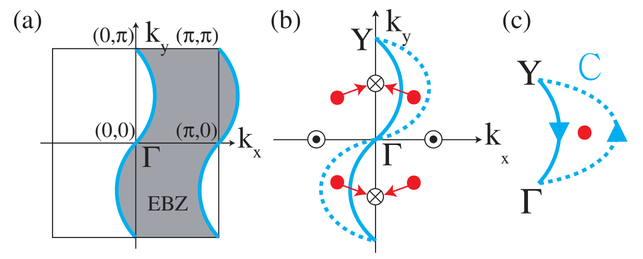

FIG. 2. (a) Two blue lines denote 1D T-invariant subsystems passing two time-reversal invariant momenta with $k_x = 0$ or $k_x = \pi$, respectively. EBZ indicates the half Brillouin zone bounded by these two T-invariant 1D subsystems. (b) A schematic figure describing the motion of WPs and the associated change in the topological invariant of a T-invariant 1D subsystem. Red dots indicate 2D WPs whose trajectories are described by red arrows. The solid (dotted) line indicates the 1D subsystem before (after) a gap closing due to the relevant WPs. Circledots and circletimes are locations where pair creation and pair annihilation of WPs happen. (c) A closed loop C encircling a 2D WP.

function centers such as $P^{j=I,II} = \sum_n^j \langle R,n|r|R,n\rangle^j$ using the Wannier function $|R,n\rangle^j = \int(dk/2\pi)e^{-ik(R-r)}|u_n^j(k)\rangle$ [21–23]. In general, P_ρ can take any real value, modulo an integer, whereas P_T is an integral quantity whose magnitude is gauge dependent. Thus, in a generic 1D T-invariant system, neither P_T, P_ρ, nor $2P^I$ can serve as a topological invariant.

However, in the presence of additional C_{2z} symmetry, $2P^I = P_T + P_\rho$ becomes a Z_2 topological invariant [14]. Namely, $2P^I$ becomes quantized and gauge-invariant modulo 2 when I_{ST} exists. Because C_{2z} makes P^I take a quantized value, either 0 or $\frac{1}{2}$ modulo an integer, $2P^I$ naturally becomes a Z_2 quantity. $2P^I$ is also proposed as a Z_2 topological invariant in a T-invariant 1D system with mirror symmetry in Ref. [24].

Now let us explain how the pair creation and pair annihilation of 2D WPs can change the Z_2 invariant Δ given by

$$\Delta = 2P^I(\pi) - 2P^I(0) - [P_\rho(\pi) - P_\rho(0)]. \quad (5)$$

In an insulating phase, since the Chern number of the whole system is zero, one can choose a continuous gauge in which

$$P_\rho(\pi) - P_\rho(0) = \int_{\mathrm{EBZ}} d^2k F(\boldsymbol{k}) = 0, \quad (6)$$

where EBZ indicates the effective half-Brillouin zone bounded by two T-invariant 1D systems defined above, and we have used that Berry curvature $F(\boldsymbol{k}) = 0$ due to I_{ST}. Thus, the change of Δ is simply given by $\delta\Delta = \delta[2P^I(\pi)] - \delta[2P^I(0)]$. Because $2P^I$ is a topological invariant, it can be changed only if an accidental gap closing happens in the relevant 1D T-invariant subsystem. In the process shown in Fig. 2(b) where 2D WPs pass through the 1D subsystem with $k_x = 0$, we have

$$\delta\Delta = -\delta[2P^I(0)] = -\frac{1}{\pi}\oint_C d\boldsymbol{k}\cdot\boldsymbol{A}(\boldsymbol{k}), \quad (7)$$

where C is a closed loop encircling one WP shown in Fig. 2(c). Since a 2D WP has π Berry phase, $\delta\Delta = 1$ ($\delta\Delta = 0$) if C encloses an odd (even) number of WPs. Hence, the Z_2 invariant Δ can be changed by 1 via partner exchange between two pairs of 2D WPs.

Model Hamiltonian.—To demonstrate the unconventional TPT, we construct a simple model Hamiltonian, a variant of the Bernevig-Hughes-Zhang (BHZ) model, which was originally proposed to describe the quantum spin Hall effect in a HgTe/CdTe quantum well [25,26]. The BHZ model is defined on a square lattice in which each site has two s orbitals $|s,\uparrow\rangle$, $|s,\downarrow\rangle$ and two spin-orbit coupled p orbitals $|p_x + ip_y,\uparrow\rangle$, $|p_x - ip_y,\downarrow\rangle$. Nearest-neighbor hopping between these four orbitals gives a tight-binding Hamiltonian given by

$$H_{\mathrm{BHZ}}(\boldsymbol{k}) = \varepsilon(\boldsymbol{k}) + d_1(\boldsymbol{k})\sigma_x s_z + d_2(\boldsymbol{k})\sigma_y + d_3(\boldsymbol{k})\sigma_z, \quad (8)$$

where $d_1(\boldsymbol{k}) + id_2(\boldsymbol{k}) = A[\sin k_x + i\sin k_y]$, $d_3(\boldsymbol{k}) = -2B[2 - M/2B - \cos k_x - \cos k_y]$, $\varepsilon(\boldsymbol{k}) = C - 2D[2 - \cos k_x - \cos k_y]$, and the Pauli matrices $\sigma_{x,y,z}$ ($s_{x,y,z}$) denote the orbital (spin) degrees of freedom. H_{BHZ} describes a QSHI (NI) when $0 < M/2B < 2$ ($M/2B < 0$). The TPT can also be understood from the energy eigenvalues of H_{BHZ}, $E(\boldsymbol{k}) = \varepsilon(\boldsymbol{k}) \pm \sqrt{d_1^2(\boldsymbol{k}) + d_2^2(\boldsymbol{k}) + d_3^2(\boldsymbol{k})}$. The energy gap closes when three equations $d_1 = d_2 = d_3 = 0$ are simultaneously satisfied, which uniquely determines the three variables $(k_x, k_y, M/B) = (0,0,0)$ when $M/B < 4$.

H_{BHZ} is invariant under inversion $P = \sigma_z$, fourfold rotation about z axis $C_{4z} = (\sigma_z + is_z)/\sqrt{2}$, twofold rotation about x, y axis $C_{2x} = i\sigma_z s_x$, $C_{2y} = is_y$, and time reversal $T = is_y K$. However, the real HgTe system lacks P and C_{4z} while retaining their product $PC_{4z}^3 \equiv S_4$ symmetry as well as T, C_{2x}, C_{2y}, and $C_{2z} = C_{4z}^2$. In fact, once P is absent, a constant term $\lambda\sigma_y s_y$ is allowed. Then, the resulting Hamiltonian $H_{\mathrm{HgTe}}(\boldsymbol{k}) = H_{\mathrm{BHZ}}(\boldsymbol{k}) + \lambda\sigma_y s_y$ is invariant under T, C_{2x}, C_{2y}, C_{2z}, and S_4. The energy eigenvalues of $H_{\mathrm{HgTe}}(\boldsymbol{k})$ are $E(\boldsymbol{k}) = \varepsilon(\boldsymbol{k}) \pm \sqrt{(\sqrt{d_1^2 + d_2^2} \pm |\lambda|)^2 + d_3^2}$. Since gap closing requires only two conditions, $d_1^2 + d_2^2 = \lambda^2$ and $d_3 = 0$, to be satisfied, one can expect a line of gapless solutions in $(k_x, k_y, M/B)$ space describing a WSM. Generally, the solution of each gap-closing condition forms a closed loop in momentum space. In Fig. 3, we plot the evolution in the shape of two loops that describe the momenta satisfying $d_1^2 + d_2^2 = \lambda^2$ and $d_3 = 0$, respectively. When these two loops overlap, the band gap closes at the momentum where the two loops touch; thus, the system becomes a WSM. We find that, when $(M/B)_{c1} < M/B < (M/B)_{c2}$, two loops overlap at eight points, indicating an emergent WSM having 8 WPs. Here $(M/B)_{c1} \equiv 4 - \sqrt{16 - 2(2\lambda/A)^2}$ and

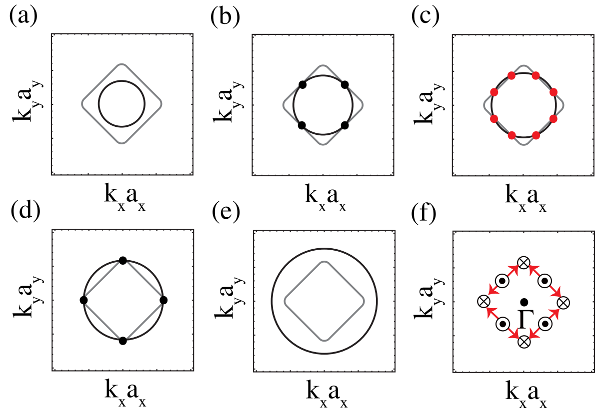

FIG. 3. Schematic figures describing the TPT in the BHZ model including an inversion breaking term. Two loops in each panel indicate the momenta where two gap-closing conditions, $d_1^2 + d_2^2 = \lambda^2$ (grey line) and $d_3 = 0$ (black line), respectively, are satisfied. (a) $M/B < (M/B)_{c1}$ relevant to a NI. (b) $M/B = (M/B)_{c1}$. (c) $(M/B)_{c1} < M/B < (M/B)_{c2}$ relevant to a WSM. Here each red dot indicates a WP. (d) $M/B = (M/B)_{c2}$. (e) $M/B > (M/B)_{c2}$ relevant to a QSHI. (f) The momentum space trajectory of WPs as M/B increases from $(M/B)_{c1}$ to $(M/B)_{c2}$. Here circledots and circletimes are the locations where, respectively, pair creation and pair annihilation of WPs happen.

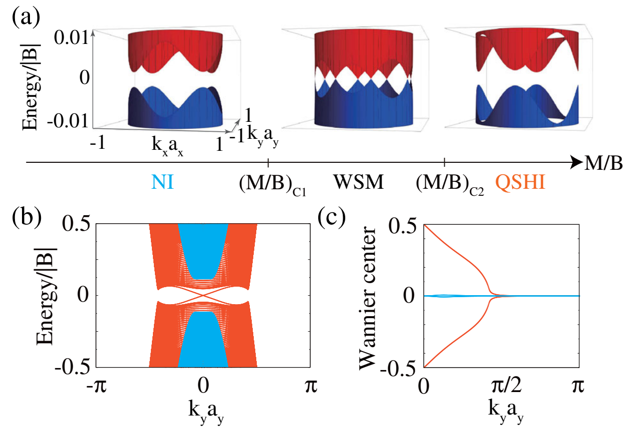

FIG. 4. (a) Evolution of the band structure across the TPT obtained from the BHZ model including the inversion breaking term with $A/B = 0.2$, $\lambda/B = 0.15$. To clarify the band structure near the gap-closing point, we set $\varepsilon(\boldsymbol{k}) = 0$. The representative band structures are calculated at $M/B = 0.595$ (NI), 0.645 (WSM), and 0.695 (QSHI). (b) Energy spectrum of a finite-size strip structure. (c) The evolution of the Wannier function centers. In (b),(c) blue and orange lines are relevant to when $M/B = 0$ (NI) and $M/B = 1.5$ (QSHI), respectively.

$(M/B)_{c2} \equiv 2 - \sqrt{4 - (2\lambda/A)^2}$. On the other hand, when $M/B < (M/B)_{c1}$ or $M/B > (M/B)_{c2}$, two loops do not overlap; thus, the system is a gapped insulator. At the critical point with $M/B = (M/B)_{c1,c2}$, the band gap closes at four points related by S_4, and each splits into two WPs in the WSM phase. This result demonstrates that the TPT in a HgTe/CdTe quantum well can be mediated by an intermediate 2D WSM. The occurrence of a semimetal phase in the HgTe/CdTe quantum well is also proposed in Ref. [10] based on symmetry analyses. Let us note that the number of gap-closing points at the critical point depends on the symmetry of the system. For instance, once S_4 symmetry is broken by applying uniaxial strain, one can observe two gap-closing points at the critical point and the intermediate WSM has four WPs (see Supplemental Material [14]). However, irrespective of the number of gap-closing points, the WSM can mediate a TPT as long as the trajectory of WPs forms a single closed loop.

To prove that the 2D WSM mediates a TPT, we should compare the Z_2 invariant Δ of two insulating phases existing when $M/B < (M/B)_{c1}$ and $M/B > (M/B)_{c2}$, respectively. For this purpose, we first compute the energy spectrum of a strip structure having a finite size along one direction. As shown in Fig. 4(b), when $M/B > (M/B)_{c2}$, one can clearly observe helical edge states localized on the sample boundary, which is absent when $M/B < (M/B)_{c1}$. Thus the system is a QSHI (NI) when $M/B > (M/B)_{c2}$ $[M/B < (M/B)_{c1}]$. For further confirmation, we directly compute Δ numerically. Because inversion symmetry is broken, one cannot use parity eigenvalues to evaluate Δ [27]. Instead, we determine Δ by computing the change of the time-reversal polarization P_T between $k_x = 0$ and $k_x = \pi$ by using Eq. (3). Because P_T is given by the difference in the Wannier function centers of Kramers pairs, one can determine Δ by examining how Wannier function centers of Kramers pairs evolve between $k_x = 0$ and $k_x = \pi$ [21,28]. As shown in Fig. 4(c), when $M/B > (M/B)_{c2}$ $[M/B < (M/B)_{c1}]$, one can see partner switching (no partner switching) of Wannier functions when k_x changes from 0 to π. Since the partner switching (no partner switching) between Wannier states indicates the change of P_T by 1 (0), one obtains $\Delta = 1$ ($\Delta = 0$) when $M/B > (M/B)_{c2}$ $[M/B < (M/B)_{c1}]$.

Discussion.—The unconventional TPT mediated by a WSM can generally occur in any 2D noncentrosymmetric system with I_{ST} symmetry. Similar to the BHZ model including an inversion breaking term, we have found that the Kane-Mele model on the honeycomb lattice including Rashba coupling also undergoes a TPT mediated by a 2D WSM when uniaxial strain is applied (see Supplemental Material [14]). Among real materials, we propose few-layer black phosphorus as another candidate system since its band gap can be controlled by electric-field breaking inversion [29]. Although there are several theoretical proposals for possible TPT in this system [30–32], the unconventional mechanism we propose has never been discussed. In fact, a recent experiment [33] has shown that the band gap of this system can be controlled by doping potassium on the surface; thus, the insulator-semimetal transition can be realized. The presence of 2D WPs in the semimetal phase has also been observed in a first-principles calculation [34]. We expect that when stronger electric field is applied to the WSM phase, even a QSHI can be obtained. For confirmation, we have studied a tight-binding model describing black phosphorus under vertical electric field, and have shown that the unconventional TPT can occur (see Supplemental Material for details [14]). Because the presence of C_{2z} with broken inversion is the only requirement for realizing the novel TPT, the same phenomenon may occur in various 2D materials with C_{2z} such as the puckered honeycomb structure of arsenene, antimonene, and bismuthene [35], the dumbbell structure of germanium-tin and stanene [36], the bismuth monobromide [37], and so forth.

We conclude with the discussion about electron correlation and disorder effects on the TPT. Although 2D WSM is perturbatively stable against weak interaction, sufficiently strong interaction can induce nontrivial physical consequences. For instance, a phase-breaking T symmetry is proposed to appear between a NI and a QSHI due to interaction [38]. In particular, at the critical point between the WSM and an insulator, because the energy dispersion becomes anisotropic, i.e., linear in one direction and quadratic in the other direction [see Eq. (2)], the density of states shows $D(E) \propto \sqrt{E}$ with the energy E, contrary to $D(E) \propto E$ in the WSM with linear dispersion in two directions. Such an enhancement of $D(E)$ makes the electron correlation and disorder cause nontrivial physical consequences. For instance, a recent renormalization group study [39] has shown that quantum fluctuation of anisotropic Weyl fermions makes the screened Coulomb interaction have spatial anisotropy, which eventually leads to marginal Fermi liquid behavior of low-energy quasiparticles. Also, in the presence of disorder, a disorder-induced new semimetal phase can appear between the insulator and WSM [40]. Understanding the interplay of electron correlation and disorder is an important problem, which we leave for future study.

J. A. was supported by Grant No. IBS-R009-D1. B.-J. Y was supported by Grant No. IBS-R009-D1, the Research Resettlement Fund for the new faculty of Seoul National University, and the Basic Science Research Program through the National Research Foundation of Korea (NRF) funded by the Ministry of Education (Grant No. 0426-20150011). We thank Keunsu Kim, Akira Furusaki, and Takahiro Morimoto for useful discussions.

*bjyang@snu.ac.kr

[1] M. Z. Hasan and C. L. Kane, Rev. Mod. Phys. **82**, 3045 (2010).
[2] X.-L. Qi and S.-C. Zhang, Rev. Mod. Phys. **83**, 1057 (2011).
[3] Y. Ando and L. Fu, Annu. Rev. Condens. Matter Phys. **6**, 361 (2015).
[4] T. H. Hsieh, H. Lin, J. Liu, W. Duan, A. Bansil, and L. Fu, Nat. Commun. **3**, 982 (2012); J. C. Y. Teo, L. Fu, and C. L. Kane, Phys. Rev. B **78**, 045426 (2008); Y. Tanaka, Z. Ren, T. Sato, K. Nakayama, S. Souma, T. Takahashi, K. Segawa, and Y. Ando, Nat. Phys. **8**, 800 (2012); P. Dziawa *et al.*, Nat. Mater. **11**, 1023 (2012); S. Xu *et al.*, Nat. Commun. **3**, 1192 (2012).
[5] S. Murakami and S.-i. Kuga, Phys. Rev. B **78**, 165313 (2008); S. Murakami, New J. Phys. **9**, 356 (2007).
[6] S. Murakami, S. Iso, Y. Avishai, M. Onoda, and N. Nagaosa, Phys. Rev. B **76**, 205304 (2007).
[7] In this Letter we call the linearly dispersing twofold (fourfold) degenerate gapless point nodes as Weyl (Dirac) points. In high-energy physics, the terms Weyl and Dirac are used to name spinor representations of the Lorentz group. Dirac representation is the irreducible representation of Clifford algebra $\{\Gamma_0,\Gamma_1,\ldots,\Gamma_d\}$ with $\{\Gamma^\mu,\Gamma^\nu\} = 2\mathrm{diag}(-1,1,\ldots,1)$, and Weyl representation is given by a restriction of it to states with fixed eigenvalue $+1$ or -1 under the action of the chirality operator $\Gamma_{d+1} \equiv i^{-(d-1)/2}\Gamma_0\Gamma_1\ldots\Gamma_d$ which can be defined only for even spacetime dimensions. Dirac representation in $(2+1)$D is a two component representation, and there is no Weyl representation in this sense. The denomination we use are analogous to the massless spinor representation of the (3+1) D Lorentz group.
[8] X. Dai, T. L. Hughes, X.-L. Qi, Z. Fang, and S. C. Zhang, Phys. Rev. B **77**, 125319 (2008).
[9] M. Knig, H. Buhmann, L. W. Molenkamp, T. L. Hughes, C.-X. Liu, X. L. Qi, and S. C. Zhang, J. Phys. Soc. Jpn. **77**, 031007 (2008).
[10] R. Winkler, L. Y. Wang, Y. H. Lin, and C. S. Chu, Solid State Commun. **152**, 2096 (2012).
[11] S. A. Tarasenko, M. V. Durnev, M. O. Nestoklon, E. L. Ivchenko, J.-W. Luo, and A. Zunger, Phys. Rev. B **91**, 081302(R) (2015).
[12] C. Fang and L. Fu, Phys. Rev. B **91**, 161105(R) (2015).
[13] C. L. Kane and E. J. Mele, Phys. Rev. Lett. **95**, 226801 (2005).
[14] See Supplemental Material at http://link.aps.org/supplemental/10.1103/PhysRevLett.118.156401, which includes Refs. [15–20], for the proof of $I_{\mathrm{ST}} = K$, and the change of topological invariant by the partner exchange of Weyl point pairs, and further application of our theory to systems other than the BHZ model.
[15] J. E. Moore and L. Balents, Phys. Rev. B **75**, 121306(R) (2007).
[16] Y. Hasegawa, R. Konno, H. Nakano, and M. Kohmoto, Phys. Rev. B **74**, 033413 (2006).
[17] S.-M. Choi, S.-H. Jhi, and Y.-W. Son, Phys. Rev. B **81**, 081407(R) (2010).
[18] A. N. Rudenko and M. I. Katsnelson, Phys. Rev. B **89**, 201408(R) (2014).
[19] P. Kumar, B. S. Bhadoria, S. Kumar, S. Bhowmick, Y. S. Chauhan, and A. Agarwal, Phys. Rev. B **93**, 195428 (2016).
[20] P. Leubner, L. Lunczer, C. Brüne, H. Buhmann, and L. W. Molenkamp, Phys. Rev. Lett. **117**, 086403 (2016).
[21] L. Fu and C. L. Kane, Phys. Rev. B **74**, 195312 (2006).
[22] B. I. Blount, Solid State Phys. **13**, 305 (1962).
[23] J. Zak, Phys. Rev. Lett. **62**, 2747 (1989).
[24] A. Lau, J. van den Brink, and C. Ortix, Phys. Rev. B **94**, 165164 (2016).
[25] B. A. Bernevig, T. L. Hughes, and S.-C. Zhang, Science **314**, 1757 (2006).

[26] M. König, S. Wiedmann, C. Brüne, A. Roth, H. Buhmann, L. W. Molenkamp, X.-L. Qi, and S.-C. Zhang, Science **318**, 766 (2007).

[27] L. Fu and C. L. Kane, Phys. Rev. B **76**, 045302 (2007).

[28] R. Yu, X. L. Qi, A. Bernevig, Z. Fang, and X. Dai, Phys. Rev. B **84**, 075119 (2011).

[29] H. Liu, A. T. Neal, Z. Zhu, Z. Luo, X. Xu, D. Tománek, and P. D. Ye, ACS Nano **8**, 4033 (2014).

[30] Q. Liu, X. Zhang, L. B. Abdalla, A. Fazzio, and A. Zunger, Nano Lett. **15**, 1222 (2015).

[31] T. Zhang, J.-H. Lin, Y.-M. Yu, X.-R. Chen, and W.-M. Liu, Sci. Rep. **5**, 13927 (2015).

[32] E. Taghizadeh Sisakht, F. Fazileh, M. H. Zare, M. Zarenia, and F. M. Peeters, Phys. Rev. B **94**, 085417 (2016).

[33] J. Kim, S. S. Baik, S. H. Ryu, Y. Sohn, S. Park, B.-G. Park, J. Denlinger, Y. Yi, H. J. Choi, and K. S. Kim, Science **349**, 723 (2015).

[34] S. S. Baik, K. S. Kim, Y. Yi, and H. J. Choi, Nano Lett. **15**, 7788 (2015).

[35] G. Zheng, Y. Jia, S. Gao, and S.-H. Ke, Phys. Rev. B **94**, 155448 (2016); C. Kamal and M. Ezawa, Phys. Rev. B **91**, 085423 (2015); S. Zhang, M. Xie, F. Li, Z. Yan, Y. Li, E. Kan, W. Liu, Z. Chen, and H. Zeng, Angew. Chem., Int. Ed. Engl. **55**, 1666 (2016); T. Nagao, J. T. Sadowski, M. Saito, S. Yaginuma, Y. Fujikawa, T. Kogure, T. Ohno, Y. Hasegawa, S. Hasegawa, and T. Sakurai, Phys. Rev. Lett. **93**, 105501 (2004).

[36] X. Chen, L. Li, and M. Zhao, RSC Adv. **5**, 72462 (2015); P. Tang, P. Chen, W. Cao, H. Huang, S. Cahangirov, L. Xian, Y. Xu, S.-C. Zhang, W. Duan, and A. Rubio, Phys. Rev. B **90**, 121408(R) (2014).

[37] J.-J. Zhou, W. Feng, C.-C. Liu, S. Guan, and Y. Yao, Nano Lett. **14**, 4767 (2014).

[38] D. I. Pikulin and T. Hyart, Phys. Rev. Lett. **112**, 176403 (2014).

[39] H. Isobe, B.-J. Yang, A. Chubukov, J. Schmalian, and N. Nagaosa, Phys. Rev. Lett. **116**, 076803 (2016).

[40] D. Carpentier, A. A. Fedorenko, and E. Orignac, Europhys. Lett. **102**, 67010 (2013).